A Journal of the Gesellschaft Deutscher Chemiker

Angewandte International Edition GDCh Chemie

www.angewandte.org

Accepted Article

Title: Tunable Electrochemical C-N versus N-N Bond Formation of Nitrogen-Centered Radicals Enabled by Dehydrogenative Dearomatization: Biological Applications

Authors: Shide Lv, Xiaoxin Han, Jian-Yong Wang, Mingyang Zhou, Yanwei Wu, Li Ma, Liwei Niu, Wei Gao, Jianhua Zhou, Wei Hu, Yuezhi Cui, and Jianbin Chen

To be cited as: *Angew. Chem. Int. Ed.* 10.1002/anie.202001510
Angew. Chem. 10.1002/ange.202001510

Link to VoR: http://dx.doi.org/10.1002/anie.202001510
http://dx.doi.org/10.1002/ange.202001510

WILEY-VCH

10.1002/anie.202001510

RESEARCH ARTICLE

WILEY-VCH

Tunable Electrochemical C-N *versus* N-N Bond Formation of Nitrogen-Centered Radicals Enabled by Dehydrogenative Dearomatization: Biological Applications

Shide Lv,[a],† Xiaoxin Han,[a],† Jian-Yong Wang,[b] Mingyang Zhou,[a] Yanwei Wu,[a] Li Ma,[a] Liwei Niu,[a] Wei Gao,[a] Jianhua Zhou,[a] Wei Hu,[a] Yuezhi Cui,[a] and Jianbin Chen*[a]

Dedication ((optional))

Abstract: Herein, an environmentally friendly electrochemical approach is reported that takes advantage of the captodative effect and delocalization effect to generate nitrogen-centered radicals (NCRs). By changing the reaction parameters of the electrode material and feedstock solubility, dearomatization enabled a selective dehydrogenative C-N *versus* N-N bond formation reaction. Hence, pyrido[1,2-*a*]benzimidazole and tetraarylhydrazine frameworks were prepared *via* a sustainable transition-metal- and exogenous oxidant-free strategy with broad generality. Bioactivity assays demonstrated that pyrido[1,2-*a*]benzimidazoles displayed antimicrobial activity and cytotoxicity against human cancer cells. Compound **21** exhibited good photochemical properties with a large Stokes shift (approximately 130 nm) and was successfully applied to subcellular imaging. A preliminary mechanism investigation and density functional theory (DFT) calculations revealed the possible reaction pathway. Interestingly, the hydrazine products could be converted into pyrido[1,2-*a*]benzimidazole cores under a complementary acidic conditions, although the former was not the intermediate en route to the latter. Consequently, this divergent synthetic route will stimulate the NCRs development in electroorganic synthesis and related biomedical sciences.

Introduction

Nitrogen-containing compounds are frequently found in natural products, pharmaceuticals, agrochemicals, and materials science. Considerable efforts have been devoted to the construction of privileged manifolds, especially *via* transition-metal-catalyzed cross-coupling and/or dehydrogenative amination strategies.[1] Free radicals play a pivotal role in biological systems and can be employed as versatile intermediates in novel reactions that would otherwise be difficult to achieve with typical ionic transformations.[2] However, compared with the well-established traditional ionic reactions for the synthesis of nitrogen-containing skeletons, the corresponding nitrogen-centered radical (NCR) strategy is in its infancy due to the highly reactive nature and short lifetime of those radicals.[3] Notably, most of the success of this strategy has strongly depended on the assistance of stannyl radicals and/or photochemistry. In sharp contrast, electrochemical studies based on NCRs have been limited thus far.[3f, 4] Two strategies have been employed to stabilize the aromatic aminyl radicals, namely, the use of captodative effects in the presence of a strong electron-withdrawing group such as an amide[3f, 4a-d] or a sulfamide group[4k-n] (**Scheme 1a**, **A**) and delocalization effects originating from diaryl amine motifs[4e-j] (**Scheme 1a**, **B**). Considering of the intriguing structure of pyridine, both the captodative effect and the delocalization effect might be achieved in one molecule. Interestingly, dearomatization of the pyridine motif can effectively proceed under electrolytic conditions.[4q, 5, 16e] The aforementioned meaningful discoveries promoted us to question whether a tunable behavior of species **C** could be achieved *via* the dearomative strategy (**Scheme 1a**, **C**).

Pyrido[1,2-*a*]benzimidazoles are an important class of heterocyclic compounds, and they display a myriad of biological activities, such as antimalarial,[6] antifungal,[7] antitumor,[8] antibacterial,[9] and antiviral,[10] as well as applications in fluorescence and dyes[11] (**Scheme 1b**). Thus, remarkable attention has been focused on their construction. For instance,

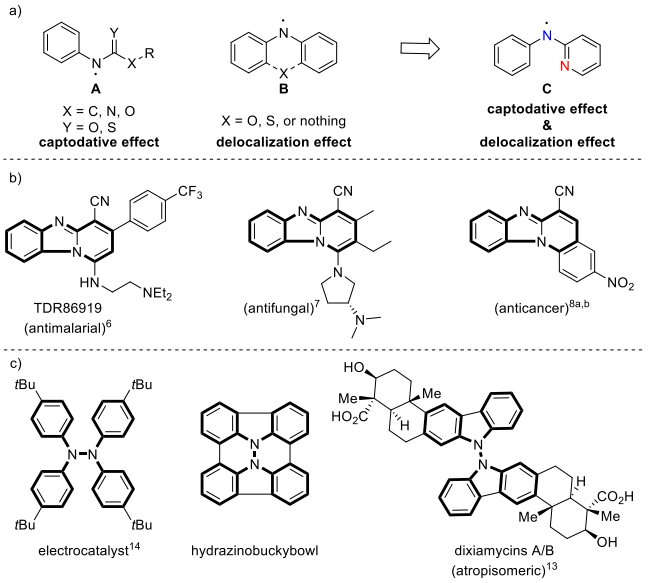

Scheme 1. Representative scaffolds of aminyl radicals, pyrido[1,2-*a*]benzimidazoles and tetraarylhydrazines.

[a] S. Lv, X. Han, Prof. Dr. M. Zhou, Y. Wu, Dr. L. Ma, Dr. L. Niu, W. Gao, Prof. Dr. J. Zhou, Prof. Dr. W. Hu, Prof. Dr. Y. Cui, Prof. Dr. J. Chen
Shandong Provincial Key Laboratory of Molecular Engineering, School of Chemistry and Pharmaceutical Engineering
Qilu University of Technology (Shandong Academy of Sciences), Jinan, 250353, P R China
E-mail: jchen@qlu.edu.cn
[b] Prof. Dr. J.-Y. Wang
School of Light Industry and Engineering
Qilu University of Technology (Shandong Academy of Sciences), Jinan, 250353, P R China
[†] These authors contributed equally to this work.

Supporting information for this article is given via a link at the end of the document.((Please delete this text if not appropriate))

10.1002/anie.202001510

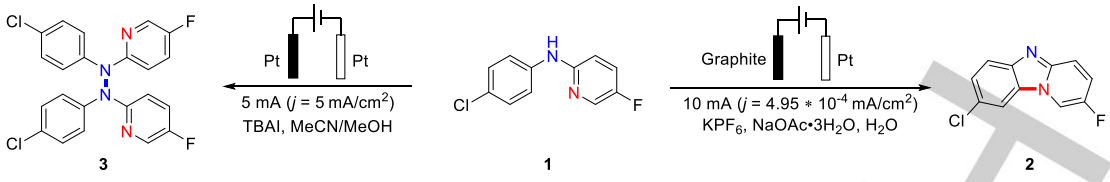

Scheme 2. Tunable electrochemical C-N *vs* N-N formation.

copper-catalyzed and/or hypervalent iodine (III)-mediated intramolecular C-H amination has been independently reported by the Zhu, Maes, and Dasgroups.[12] In addition, tetraarylhydrazines are unique motifs in the natural product dixiamycins A and B[13] and can be employed as electrocatalysts[14] (**Scheme 1c**). Conventional transition-metal-catalyzed oxidative coupling of secondary amines with oxidants is the primary procedure for their preparation.[15] In view of these privileged structures and our interests[16] in organic electrochemistry,[17] we envision that by controlling one of the key factors in electrochemistry, namely, the current density, the distinctive target compound might be furnished in a tunable manner via transition-metal- and exogenous oxidant-free electrochemical dehydrogenative NCR strategies. The hypothesis was based on the principle that the current density is proportional to the reaction rate at the electrode surface, and hence correlates to the concentration of the reactive intermediate species.

Results and discussion

With this idea in mind, we identified two separate optimal systems for electrochemical intramolecular C-N and intermolecular N-N oxidative coupling reactions with *N*-(4-chlorophenyl)-5-fluoropyridin-2-amine **1** as the feedstock (**Scheme 2,** see Table S2 and S3). First, the generality of the cyclization product was tested (**Table 1**, standard condition A). As shown, a broad spectrum of functional groups was tolerated with good to quantitative efficiency. Specifically, electron-donating groups, such as alkyl (**4**, **5**, **15**, **16**), ether (**6**, **7**, **17**, **18**), and thioether groups (**9**), and electron-withdrawing groups including fluoro (**8**, **22**, **23**, **25**, **28**, **29**), chloro (**2**, **22**, **26**, **28**), bromo (**27**), and trifluoromethoxy (**10,** **19**) moieties reacted smoothly in the aqueous system. Interestingly, the groups that was electrochemical oxidative and reductive labile were intact in moderate yields. This observation was exemplified by the amino (**20**, **21**), and thioether groups for the electrochemical oxidative moieties and by the aldehyde (**32**), ketone (**31**), and ester (**11**, **33**) groups for the reductive lable moieties. Regarding the steric hindrance, the *meta*-substituted starting materials exclusively favored the less steric position (**16**, **22**, **23**, **28**, **29**). Moreover, *ortho*-phenyl (**24**) was formed selectively in our system accomplishing the desired pyrido[1,2-*a*]benzimidazole core instead of the carbazole unit. The naphthalene site could also be cyclized with moderate efficiency (**34**). In some cases, methyl thioglycolate[18] or NaI[5] was added to improve the yields.

Next, we moved to the substrate scope of the N-N bond

Table 1. Generality of the intramolecular C-N bond cyclization.

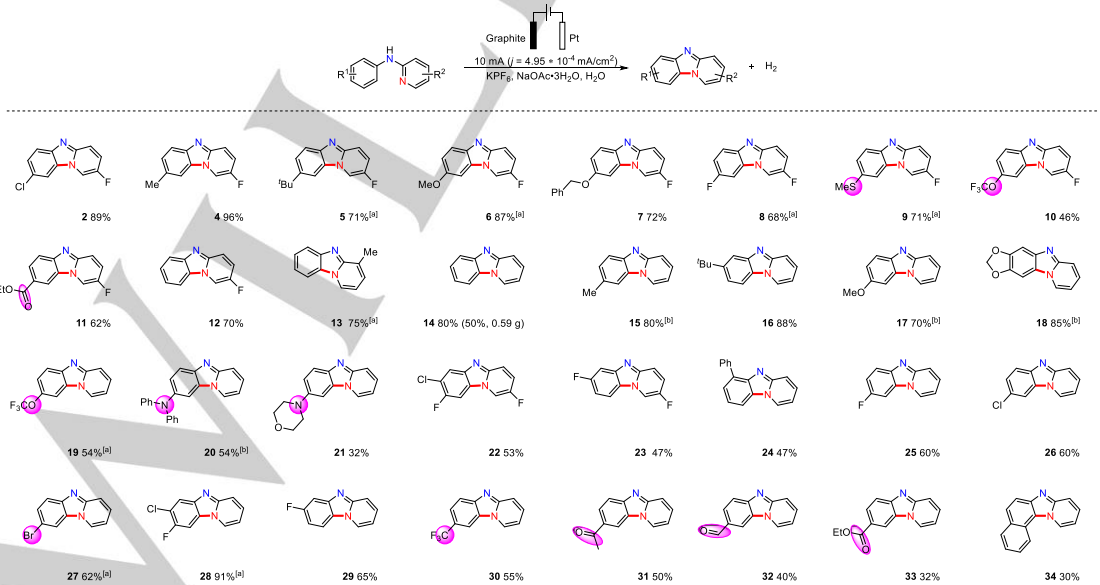

Reaction condition A: Substance (0.2 mmol), KPF_6 (2 equiv.), $NaOAc{\cdot}3H_2O$ (2 equiv.), a graphite rod (ϕ 10 mm) as the anode, a Pt sheet (1 × 1 cm) as the cathode, H_2O (5 mL), 10 mA (j = 4.95 × 10^{-4} mA/cm^2), N_2, 100 °C, 16 h. [a] with $HSCH_2CO_2Me$ (10 mol%) and [b] with NaI (1.2 equiv.).

Table 2. Generality of the intermolecular N-N bond formation reaction.

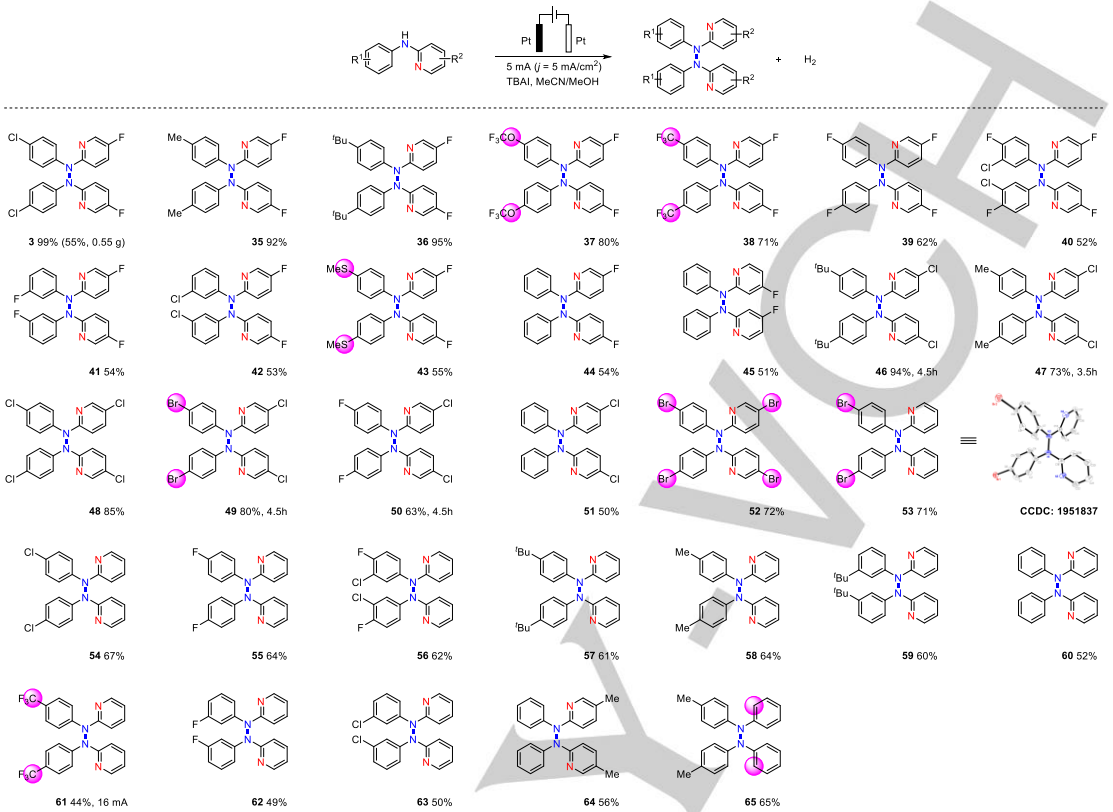

Reaction condition B: Substance (0.25 mmol), TBAI (2 equiv.), a Pt sheet (1 × 1 cm) as the anode and cathode, MeCN-MeOH (7-0.5 mL), 5 mA (j = 5 mA/cm^2), N_2, 60 °C, 10 h.

formation part (**Table 2**, standard condition B). Once again, the electronic and steric effects on the benzene ring were examined. Electron-rich groups such as an alkyl group (**35**, **36**, **46, 47, 57, 58, 59**) and electron-deficient groups such as fluoro (**39**, **40**, **41, 50, 55, 56, 62**), chloro (**3**, **40, 42, 48, 54, 56, 63**), bromo (**49, 52, 53**), and trifluoromethyl (**38, 61**) moieties were compatible. Electrochemically active thioether (**43**) was also furnished in moderate yield. Particularly, the intact bromo group provides an orthogonal reactive handle for further transition-metal-catalyzed cross-coupling reactions. In terms of the substitutents on the pyridine ring, the fluoro (**3**, **35-45**), chloro (**46-51**), bromo (**52**), and methyl (**64**) groups worked successfully. Additionally, diaryl amine (**65**) produced the corresponding hydrazine with acceptable efficiency. Fortunately, a single crystal of **53** was obtained, and thus, all the structures of the N-N coupling products were unambiguously determined. Considering the practicability of these newly developed protocols, gram-scale reactions were conducted, although diminished yields were observed [19] (see supporting information Figure S4 and S5).

Preliminary mechanism investigation

To obtain insight into the reaction mechanism, a number of control experiments (**Figure 1**) and cyclic voltammetry (CV, **Figure 2**) analyses were conducted. Electrolysis of a methyl-substituted amine resulted in almost no product (**Eq. 1**). This observation highlighted the importance of the free N-H moiety. Importantly, deprotonation of the free N-H starting material by a base *i.e.*, hydroxide, was validated by the nuclear magnetic resonance (NMR, Figure S6) and CV results (green line **1** + tetrabutylammonium hydroxide (TBAOH) *vs* pink line **1**, **Figure 2a**). Clearly, the oxidative peak potential for the nitrogen anion (green line, E_p = 0.44 V *vs* SCE) was remarkably lower than that of the corresponding starting material **1** (pink line, E_p = 1.22 V *vs* SCE, **Figure 2a**). The addition of radical scavengers such as 2,2,6,6-teramethyl-1-piperidinyloxy (TEMPO) or butylated hydroxytoluene (BHT) under the standard conditions A or B led to significant inhibition (**Eq. 2** and **4**). Remarkably, cross-coupling product **66** was accompanied by two other homocoupling products **36** and **55**, in a ratio of approximately of 1: 1: 1 when an equal molar substance was present. Furthermore, selective cross-coupling of free radicals is highly desirable.[20] Under standard condition B, the cross-coupling of compound **66** could be significantly improved by simply adding 5 equivalents of one substance (**Eq. 5**). Because of the relatively low peak potential (red line, E_p = 0.75V *vs* SCE, **Figure 2a**) in MeCN/MeOH, the direct oxidation of the iodide anion is operative. Interestingly, only compound **3** was afforded in 73% yield when the constant potential electrolysis was set at 0.75 V *vs* SCE, corresponding to the anodic oxidation of iodide anions (**Eq. 6**). Taken together, these data substantially corroborated that the nitrogen-centered radical intermediate was involved in

the process. Notably, an inverse secondary kinetic isotope effect (*KIE* = 0.89) under condition **A** was measured (**Eq. 3**). The data were consistent with the configuration change in the carbon center from sp^2 to sp^3 and demonstrated that C-H bond cleavage was not involved in the amination step. Markedly, this result was completely different from the Cu-catalyzed C-H amination reaction.[12a] Then, we investigated the electrochemical behavior of compounds **1**, **2**, and **3** via CV. Interestingly, a reversible cyclic voltammogram for **3** was observed whereas a completely irreversible result was found for **1**; however, almost no oxidative peak was observed for **2** in the potential window of interest (**Figure 2b**).

Density functional theory (DFT)[21] was used to explain the differences in enegy values for the reaction steps of interest (**Scheme 3**). Once nitrogen radical **B** was formed, -91.06 kJ/mol (at the B3LYP/6-311++G(d,p) level) was released when the intermolecular N-N homocoupling reaction took place. Nevertheless, the intramolecular C-N annulation was complicated. The energy barrier for the transition state (TS1) indicated that nitrogen radical attack of the aryl ring was an endothermic step and generated radical **D**. At this point, the enegy for the anodic heterogenous oxidation at the electrode surface of **D** affording species **E** was significantly lower than that of the homogenous oxidation reaction in bulk solution (pink line *vs* blue line, **Scheme 3**). Deprotonation of **E** in the presence of hydroxide furnished final product **14** in an exothermic step.

Despite the evidence for the homogenous bulk chemical process, the selectivity was still not explained. Hence, we focused on the electrode materials. A commercially available graphite rod was employed as the anode in condition A and the surface area was determined to be 2.022 m^2/g (see Figure S13). The mesoporous structure allows the organic component to easily diffuse to the electrode surface. Thus, the corresponding current density was calculated to be 4.95×10^{-4} mA/cm^2, which was approximately one ten thousandth to that of the platinum anode, as in condition B. Moreover, the starting material has poor solubility in water whereas it is totally soluble in an organic medium. The above reaction parameters ultimately led to a difference in the concentration of NCR **B**. In addition, the graphite electrode exhibited a greater paramagnetic nature than the other tested electrode, resulting in increased attraction of the radical species to the graphite surface, thereby promoting oxidation of the second electron.[17a, r, 22]

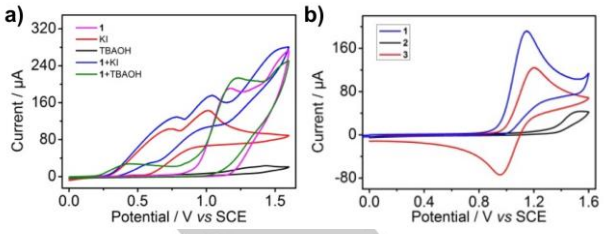

Figure 2. CV analysis. Substrate (0.01 mol/L), $LiClO_4$ (0.1 mol/L), graphite carbon (GC) as the working electrode, Pt wire as the counter electrode, SCE as the reference electrode, scan rate: 100 mV/s. a) in MeCN/MeOH (14:1); b) in MeCN.

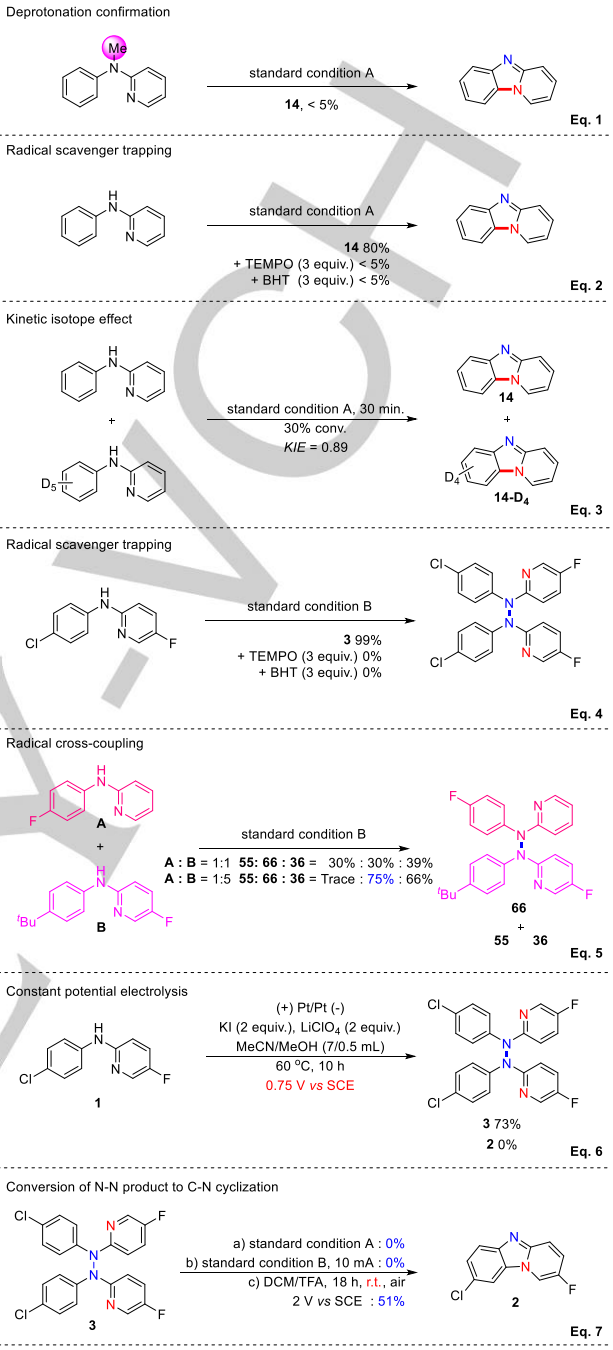

Figure 1. Control experiments.

Based on the preliminary mechanism investigation, two putative reaction pathways were proposed, as shown in **Scheme 3**. The first pathway for generating NCR **B** is the halide-mediated pathway, namely, the anodic oxidation of iodide anions accompanied with the following homolytic cleavage of the N-I bond. The second one is the direct oxidation of the nitrogen anion species **A** originating from the deprotonation of the free N-H feedstock by an electrochemically generated base. Under condition B, the good substrate solubility and the relatively high

current density from the platinum anode resulted in a sufficient concentration of NCR **B** which benefited the N-N coupling pathway. However, under condition A, an extremely low concentration of nitrogen radicals was generated. To meet the current demand, the formal dearomative isomerization of **B** to **C** along with the ensuing intramolecular nitrogen radical attack of the aryl ring supplied species **D**. Further heterogeneous oxidation of **D** on the graphite anode surface took place, thereby giving cation species **E**; subsequent deprotonation in the presence of a base eventually delivered the formal 2e oxidation scaffold **14**.[23] Finally, hydrogen evolution was responsible for the cathodic half reaction which was confirmed by gas chromatography (GC) analysis (see Figure S14).

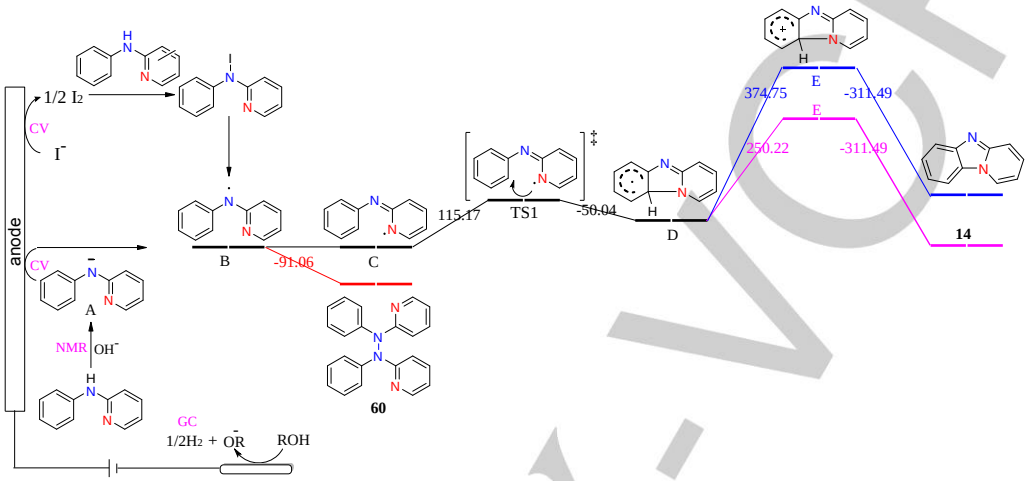

Scheme 3. Putative mechanism.

Conversion of compound 3 to 2

We questioned whether the N-N product was the intermediate en route to the C-N cyclized product. This possibility was ruled out based on the control experiment in **Eq. 7a**. Stimulated by the fact that potassium hexafluorophosphate (KPF_6) is hydrolyzed in water to make an acidic solution, we controversially performed electrolysis in an acidic medium (**Eq. 7c**)[24]. Surprisingly, compound **2** was furnished with moderate efficiency at 2 V *vs* SCE by the electrolysis of N-N product **3** in a strong acidic environment (standard condition C)**.** This discovery elucidated the reason for the failure, as exhibited in **Eq. 7a** which was ascribed to the weak acidity. Inspired by this result, several transformations were set up, as shown in **Table 3**, to consider a complementary route from the N-N structure to C-N fragments.

Table 3. Transformation of N-N compounds to C-N products.

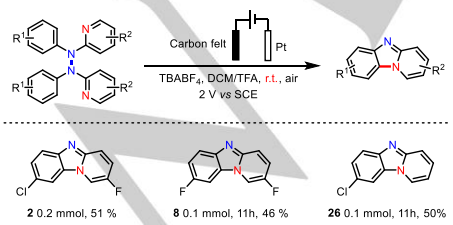

Reaction condition C: Substance (0.1-0.2 mmol), $TBABF_4$ (5 equiv.), carbon felt (1 × 1 × 0.3 cm) as the anode, a Pt sheet (1 × 1 cm) as the cathode, DCM-TFA (4.5-0.5 mL), 2 V *vs* SCE, air, r.t., 18 h.

Table 4. Bioactivity of the pyrido[1,2-*a*]benzimidazole compounds.

Compounds	Inhibition Ratio/%
	Staphylococcus aureus ATCC-6538
15	55.31 ± 1.49
	Saccharomyces cerevisiae
34	49.37 ± 5.39
	Hepatocarcinoma cell line HepG2
2	38.24 ± 4.99
8	49.16 ± 5.97
29	42.99 ± 17.57
	Melanoma cell line A375
8	53.31 ± 3.57
30	35.76 ± 11.61
	Cervix adenocarcinoma HeLa cells
12	43.90 ± 2.05

Photochemical properties and biological applications

In terms of the biological activity and fluorescence properties of pyrido[1,2-*a*]benzimidazole heterocyclic

compounds,[6-11] applications in related areas were also evaluated. First, the antimicrobial activity and cytotoxicity against human cancer cells were tested. Several compounds showed high activity. For instance, compounds **15**, **34**, and **12** could inhibit the growth of cells by 55%, 49%, and 44%, respectively. Moreover, *Staphylococcus aureus*, *Saccharomyces cerevisiae*, and cervix adenocarcinoma HeLa compounds **8** and **29** inhibited the hepatocarcinoma cell line HepG2 by more than 42%. Furthermore, compound **8** could also inhibit melanoma cell line A375 by 53%.

Second, compound **21** exhibited strong fluorescence enhancement with a large Stokes shift[25] (approximately 130 nm) at different concentrations, making it potentially applicable in subcellular imaging (**Figure 3**). Morpholine was treated as a target group of lysosomes, thus increasing the compound **21** distribution in lysosomes. To investigate the subcellular localization ability, compound **21** with the commercial lysosomal tracker LysoTracker red was applied in HeLa cells. As shown in **Figure 4**, the fluorescence signal from the green channel overlaid very well with that of LysoTracker red. Moreover, the fluorescent intensity of the green channel and red channel is well correlated with a highly overlapping Pearson´s coefficient of 0.80 and an overlapping Mander´s coefficient of 0.81. Therefore, the compound **21** was well located in the lysosomes of living cells.

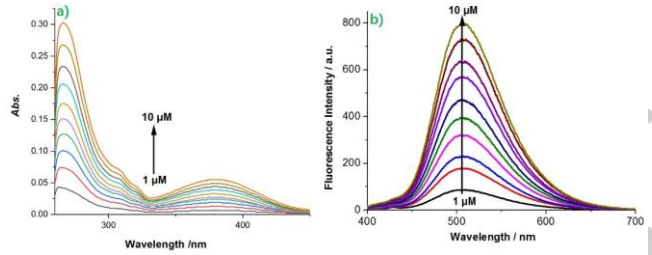

Figure 3. UV-vis absorption spectra and fluorescence emission spectra of compound **21** in DMF.

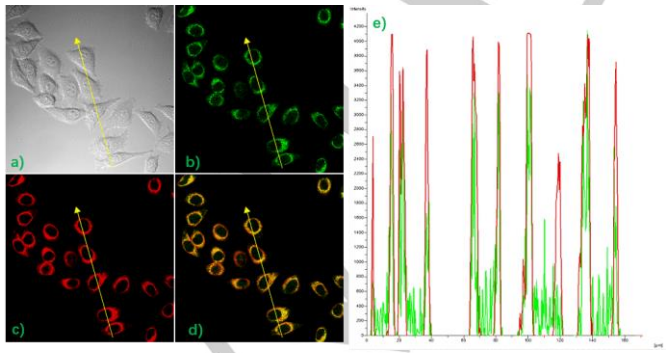

Figure 4. Brightfield and fluorescence images of HeLa cells stained with compound **21** (10 μM) and LysoTracker red. a) Brightfield image, b) with **21**, c) from the red channel (lysosome staining), d) an overlay of brighfield, green and red channels, and e) intensity profile of the linear region of interest across in the HeLa cell costained with LysoTracker red and **21**.

Conclusion

In summary, based on the captodative effect and delocalization effect, an electrochemical tunable methodology from readily available feedstock was presented, providing easy access to intermolecular N-N coupling and intramolecular C-N bond formation architectures. By changing the reaction parameters including the anode material and solvent, a considerable difference in the nitrogen radical concentration could be established. Generally, a high concentration of NCR benefits the radical N-N coupling route, while a low concentration of NCRs is further oxidized to formal dearomatization 2e oxidation products. Alternatively, conversion of the hydrazine product to pyrido[1,2-*a*]benzimidazole cores was also viable under acidic conditions, although the former was not the intermediate en route to the latter. The transition-metal- and exogenous-free features of this protocol highlight the user-friendly and sustainable nature of the newly developed organic electrolysis method. Biological evaluation demonstrated the potential application of our products, including the use of their antimicrobial and antitumor activities. The photochemical properties revealed that compound **21** was suitable for cell labeling with a large Stokes shift (approximately 130 nm); furthermore, lysosomal fluorescence imaging was realized in living cells. On the basis of these advantages, the newly developed approach represents an ideal strategy for divergent synthesis approaches, and could potentially be useful in chemistry, biomedicine and materials science.

Acknowledgements

We greatly appreciate the financial support from the National Natural Science Foundation of China (Nos. 21801144, 81872744, 51602164), the Youth Innovative Talents Recruitment and Cultivation Program of Shandong Higher Education, the Natural Science Foundation of Shandong Provincie (No. ZR2018BB017), Qilu University of Technology (Shandong Academy of Sciences, No. 0412048811), and the Program for Scientific Research Innovation Team in Colleges and Universities of Shandong Province.

Keywords: nitrogen-centered-radicals •dearomatization • dehydrogenative • electrosynthesis • tunable

[1] a) P. Ruiz-Castillo, S. L. Buchwald, *Chem. Rev.* **2016**, *116*, 12564-12649; b) J. F. Hartwig, *Acc. Chem. Res.* **2008**, *41*, 1534-1544; c) C.-Y. Huang, H. Kang, J. Li, C.-J. Li, *J. Org. Chem.* **2019**, *84*, 12705-12721. d) Y. Park, Y. Kim, S. Chang, *Chem. Rev.* **2017**, *117*, 9247-9301; e) C. Sambiagio, S. P. Marsden, A. J. Blacker, P. C. McGowan, *Chem. Soc. Rev.* **2014**, *43*, 3525-3550.

[2] *Radicals in Organic Synthesis, 1st ed.*; P. Renaud, M. P. Sibi, Eds. Wiley-VCH Verlag GmbH: Weinheim, Germany, **2001**.

[3] For selected reviews on nitrogen-centered radicals, please see: a) S. Z. Zard, *Chem. Soc. Rev.* **2008**, *37*, 1603-1618; b) J.-R. Chen, X.-Q. Hu, L.-Q. Lu, W.-J. Xiao, *Chem. Soc. Rev.* **2016**, *45*, 2044-2056; c) T. Xiong, Q. Zhang, *Chem. Soc. Rev.* **2016**, *45*, 3069-3087; d) M. D. Karkas, *ACS Catal.* **2017**, *7*, 4999-5022; e) H. Jiang, A. Studer, *CCS*

Chem. **2019**, *1*, 38-49; f) P. Xiong, H.-C. Xu, *Acc. Chem. Res.* **2019**, *52*, 3339-3350.

[4] For selected examples, please see: a) A. Kehl, V. M. Breising, D. Schollmeyer, S. R. Waldvogel, *Chem. Eur. J.* **2018**, *24*, 17230-17233. b) A. A. Folgueiras-Amador, X.-Y. Qian, H.-C. Xu, T. Wirth, *Chem, Eur. J.* **2018**, *24*, 487-491. c) T. Gieshoff, A. Kehl, D. Schollmeyer, K. D. Moeller, S. R. Waldvogel, *J. Am. Chem. Soc.* **2017**, *139*, 12317-12324; d) T. Gieshoff, D. Schollmeyer, S. R. Waldvogel, *Angew. Chem. In. Ed.* **2016**, *55*, 9437-9440; e) B. R. Rosen, E. W. Werner, A. G. O'Brien, P. S. Baran, *J. Am. Chem. Soc.* **2014**, *136*, 5571-5574; f) S. R. Waldvogel, B. Janza, *Angew. Chem. In. Ed.* **2014**, *53*, 7122-7123; g) Y.-C. Wu, S.-S. Jiang, R.-J. Song, J.-H. Li, *Chem. Commun.* **2019**, *55*, 4371-4374; h) K. Liu, S. Tang, T. Wu, S. Wang, M. Zou, H. Cong, A. Lei, *Nat. Common.* **2019**, *10*, 639; i) S. Tang, S. Wang, Y. Liu, H. Cong, A. Lei, *Angew. Chem. Int. Ed.* **2018**, *57*, 4737 -4741; j) E. Feng, Z. Hou, H.-C. Xu, *Chin. J. Org. Chem.* **2019**, *39*, 1424-1428; k) C. Liu, Q. Jiang, Y. Lin, Z. Fang, K. Guo, *Org. Lett.* **2019**, 10.1021/acs.orglett.9b04141. l) F. Wang, S. S. Stahl, *Angew. Chem. Int. Ed.* **2019**, *58*, 6385-6390. m) P. Nikolaienko, M. Jentsch, A. P. Kale, Y. Cai, M. Rueping, *Chem. Eur. J.* **2019**, *25*, 7177-7184. n) X. Hu, G. Zhang, F. Bu, L. Nie, A. Lei, *ACS Catal.* **2018**, *8*, 9370-9375. o) S. Zhang, L. Li, M. Xue, R. Zhang, K. Xu, C. Zeng, *Org. Let.* **2018**, *20*, 3443-3446; p) X. Hu, G. Zhang, L. Nie, T. Kong, A. Lei, *Nat. Common.* **2019**, *10*, 5467; q) Y. Li, Z. Ye, N. Chen, Z. Chen, F. Zhang, *Green Chem.* **2019**, *21*, 4035-4039; r) S. Tang, L. Zeng, A. Lei, *J. Am. Chem. Soc.* **2018**, *140*, 13128-13135; s) J. Chen, W.-Q. Yan, C. M. Lam, C.-C. Zeng, L.-M. Hu, R. D. Little, *Org. Lett.* **2015**, *17*, 986-989; t) J. Wu, Y. Zhou, Y. Zhou, C.-W. Chiang, A. Lei, *ACS Catal.* **2017**, *7*, 8320-8323; u) Y. Qiu, J. Struwe, T. H. Meyer, J. C. A. Oliveira, L. Ackermann, *Chem. Eur. J.* **2018**, *24*, 12784-12789.

[5] a) J.-S. Li, X.-Y. Xie, P.-P. Yang, S. Jiang, L. Tao, Z.-W. Li, C.-H. Lu, W. D. Liu, *Adv. Synth. Cat.* **2019**, DOI: 10.1002/adsc.201901290; b) P. Xu, H.-C. Xu, *ChemElectroChem* **2019**, *6*, 4177-4179.

[6] A. J. Ndakala, R. K. Gessner, P. W. Gitari, N. October, K. L. White, H. Alan, F. Foluke, D. M. Shackleford, K. Marcel, Y. Clive, S. A. Charman, K. Chibale, *J. Med. Chem.* **2011**, *54*, 4581-4589.

[7] P H. Takeshita, J. Watanabe, Y. Kimura, K. Kawakami, H. Takahashi, M. Takemura, A. Kitamura, K. Someya, K. Nakajima, *Bioorg. Med. Chem. Lett.* **2010**, *20*, 3893-3896.

[8] a) N. Perin, L. Uzelac, I. Piantanida, G. Karminski-Zamola, M. Kralj, M. Hranjec, *Bioorg. Med. Chem.* **2011**, *19*, 6329-6339; b) M. Hranjec, I. Piantanida, M. Kralj, L. Suman, K. Pavelı, G. Karminski-Zamola, *J. Med. Chem.* **2008**, *51*, 4899-4910; c) M. Hranjec, M. Kralj, I. Piantanida, M. Sed, L. Suman, K. Pavelı, G. Karminski-Zamola, *J. Med. Chem.* **2007**, *50*, 5696-5711; d) M. Dupuy, F. Pinguet, O. Chavignon, J.-M. Chezal, J.-C. Teulade, J.-P. Chapat, Y. Blache, *Chem. Pharm. Bull.* **2001**, *49*, 1061-1065; e) E. Badaway, T. Kappe, *Eur. J. Med. Chem.* **1995**, *30*, 327-332.

[9] M. Hammad, A. Mequid, M. E. Ananni, N. Shafik, *Egypt. J. Chem.* **1987**, *29*, 5401.

[10] S. K. Kotovskaya, Z. M. Baskakova, V. N. Charushin, O. N. Chupakhin, E. F. Belanov, N. I. Bormotov, S. M. Balakhnin, O. A. Serova, *Pharm. Chem. J.* **2005**, *39*, 574-578.

[11] a) J.-S. Bae, D.-W. Lee, D.-H. Lee, D.-S. Jeong (LG Chem. Ltd, Seoul), WO2007011163A1, **2007**; b) R. Erckel, D. Gunther, H. Fruhbeis (Hoechst AG., Frankfurt), DE2640760A1, **1978**;[Chem. Abstr. **1978**, *89*, 7595]; c) E. Schefzcik (BASF AG., Ludwigshafen), DE2701659A1, **1978**; d) J. Denhert, G. Lamm (BASF AG., Ludwigshafen), DE2022817, **1972**.

[12] a) H. Wang, Y. Wang, C. Peng, J. Zhang, Q. Zhu, *J. Am. Chem. Soc.* **2010**, *132*, 13217-13219; b) K.-S. Masters, T. R. M. Rauws, A. K. Yadav, W. A. Herrebout, B. Van der Veken, B. U. W. Maes, *Chem. Eur. J.* **2011**, *17*, 6315-6320; c) Y. He, J. Huang, D. Liang, L. Liu, Q. Zhu, *Chem. Commun.* **2013**, *49*, 7352-7354; d) D. N. Rao, S. Rasheed, R. A. Vishwakarma, P. Das, *RSC Adv.* **2014**, *4*, 25600-25604.

[13] For a review on natural products that contain N-N bonds, see: a) L. M. Blair, J. Sperry, *J. Nat. Prod.* **2013**, *76*, 794-812; b) Q. Zhang, A. Mandi, S. Li,; Y. Chen, W. Zhang, X.Tian, H. Zhang, H. Li, W. Zhang, S. Zhang, J. Ju, T. Kurtan, C. Zhang, *Eur. J. Org. Chem.* **2012**, *27*, 5256-5262; c) Z. Xu, M. Baunach, L. Ding, C. Hertweck, *Angew. Chem. Int. Ed.* **2012**, *51*, 10293-10297.

[14] Z. W. Hou, Z. Y. Mao, Y. Y. Melcamu, X. Lu, H.-C. Xu, *Angew. Chem. Int. Ed.* **2018**, *57*, 1636-1639.

[15] For selected examples, please see: a) M. C. Ryan, J. R. Martinelli, S. S. Stahl, *J. Am. Chem. Soc.* **2018**, *140*, 9074-9077; b) R. F. Fritsche, G. Theumer, O. Kataeva, H. J. Knolker, *Angew Chem. Int. Ed.* **2017**, *56*, 549-553; c) C. B. R. Reddy, S. R. Reddy, S. Naidu, *Catal. Commun.* **2014**, *56*, 50-54; d) Y. Zhu, Y. Shi, *Org. Lett.* **2013**, *15*, 1942-1945; e) X.-M. Yan, Z.-M. Chen, F.Yang, Z.-Z. Huang, *Synlett.* **2011**, *2011*, 569-572. One electrochemical version has been reported, please see ref. 4j: Notably, only one example of *N*-aryl-2-aminopyridine has been listed. Nevertheless, it deserves to expand the substrate scope due to the importance of the pyridine-containing products. Actually, the condition employed in this work is different with the reported system. Most importantly, we want to identify the original of the chemoselectivity between C-N and N-N bonds formation from the same starting material.

[16] a) J. Chen, S. Lv, S. Tian, *ChemSusChem*. **2019**, *12*, 115-132; b) S. Tian, X. Jian, L. Wang, B. Li, S. Liu, L. Ma, W. Gao, Y. Wei, J. Chen, *ChemCommon*. **2019**, *55*, 12104-12107; c) X. Han, K. Wang, G. Zhang, W. Gao, J. Chen, *Adv. Synth. Catal.* **2019**, *361*, 2804-2824; d) S. Tian, S. Lv, X. Jian, L. Ma, B. Li, G. Zhang, W. Gao, Y. Wei, J. Chen, *Adv. Synth. Catal.* **2019**, *361*, 5626-5633; e) S. Lv, G. Zhang, J. Chen, W. Gao, *Adv. Synth. Catal.* **2019**, DOI: 10.1002/adsc.201900750; f) G. Zhang, Q. Xu, Y. Liu, Q. Qin, J. Zhang, K. Qi, J. Chen, Z. Wang, K. Zheng, K. Swierczek, W. Zheng, *Electrochim. Acta*. **2020**, *332*, 135500; g) P. Zhang, J. Chen, W. Gao, Y. Xiao, C. Liu, S. Xu, X. Yan, D. Qin, *Molecules*, **2019**, *24*, 696.

[17] For selected reviews, please see: a) C. Kingston, M. D. Palkowitz, Y. Takahira, J. C. Vantourout, B. K. Peters, Y. Kawamata, P. S. Baran, *Acc. Chem. Res.* **2019**, DOI: 10.1021/acs.accounts.9b00539; b) M. Yan, Y. Kawamata, P. S. Baran, *Angew. Chem. Int. Ed.* **2018**, *57*, 4149-4155; c) J. L. Rockl, D. Pollok, R. Franke, S. R. Waldvogel, *Acc. Chem. Res.* **2019**, DOI: 10.1021/acs.accounts.9b00511. d) S. R. Waldvogel, S. Lip, M. Selt, B. Riehl, C. J. Kampf, *Chem. Rev.* **2018**, *118*, 6706-6765; e) J. Jiang, K. Xu, C. Zeng, *Chem. Rev*. **2018**, *118*, 4485-4540; f) M. D. Karkas, *Chem. Soc. Rev*. **2018**, *47*, 5786-5865; g) N. Sauermann, T. H. Meyer, Y. Qiu, L. Ackermann, *ACS Catal*. **2018**, *8*, 7086-7103; h) G. S. Sauer, S. Lin, *ACS Catal.* **2018**, *8*, 5175-5187; i) S. Tang, Y. Liu, A. Lei, *Chem.* **2018**, *4*, 27-45; j) Q.-L. Yang, P. Fang, T.-S. Mei, *Chin. J. Chem*. **2018**, *36*, 338-352; k) M. Yan, Y. Kawamata, P. S. Baran, *Chem. Rev.* **2017**, *117*, 13230-13319; l) E. J. Horn, B. R. Rosen, P. S. Baran, *ACS Cent. Sci*. **2016**, *2*, 302-308; m) R. Francke, R. D. Little, *Chem. Soc. Rev*. **2014**, *43*, 2492-2521; n) J. I. Yoshida, K. Kataoka, R. Horcajada, A. Nagaki, *Chem. Rev*. **2008**, *108*, 2265-2299; o) J. M.Savéan, *Chem. Rev.* **2008**, *108*, 2348-2378; p) J. B. Sperry, D. L. Wright, *Chem. Soc. Rev*. **2006**, *35*, 605-621; q) A. Jutand, *Chem. Rev*. **2008**, *108*, 2300-2347; r) Q. Jing, K. D. Moeller, *Acc. Chem. Res.* **2019**, DOI: 10.1021/acs.accounts.9b00578; s) M. C. Leech, K. Lam, *Acc. Chem. Res.* **2019**, DOI: 10.1021/acs.accounts.9b00586; t) J. L. Röckl, D. Pollok, R. Franke, S. R. Waldvogel, *Acc. Chem. Res.* **2019**, DOI: 10.1021/acs.accounts.9b00511; u) K.Yamamoto, M. Kuriyama, O. Onomura, *Acc. Chem. Res.* **2019**, DOI: 10.1021/acs.accounts.9b00513. For selected examples, please see: a) J. Xiang, M. Shang, Y. Kawamata, H. Lundberg, S. H. Reisberg, M. Chen, P. Mykhailiuk, G. Beutner, M. R. Collins, A. Davies, M. D. Bel, G. M. Gallego, J. E. Spangler, J. Starr, S. Yang, D, G. Blackmond, P. S. Baran, *Nature.* **2019**, *573*, 398-402; b) B. K. Peters, K. X. Rodriguez, S. H. Reisberg, S. B. Beil, D. P. Hickey, Y. Kawamata, M. Collins, J. Starr, L. Chen, S. Udyavara, K. Klunder, T. J. Gorey, S. L. Anderson, M. Neurock, S. D. Minteer, P. S. Baran, *Science*. **2019**, *363*, 838-845; c) E. J. Horn, B. R. Rosen, Y. Chen, J. Tang, K. Chen, M. D. Eastgate, P. S. Baran, *Nature*. **2016**, *533*, 77-81; d) N. Fu, G. S. Sauer, A. Saha, A. Loo, S. Lin, *Science*. **2017**, *357*, 575-579; e) C. J. Bondue, F. Calle-Vallejo, M. C.

Figueiredo, M. T. M. Koper, *Nat. Catal.* **2019**, *2*, 243-250; f) T.-J. He, Z. Ye, Z. Ke, J.-M. Huang, *Nat. Common.* **2019**, *10*, 833; g) X. Huang, Q. Zhang, J. Lin, K. Harms, E. Meggers, *Nat. Catal.* **2018**, *2*, 34-40; h) C. Y. Cai, H. C. Xu, *Nat. Common*. **2018**, *9*, 3551-3558; i) S. R. Waldvogel, S. Mohle, *Angew. Chem. Ind. Ed.* **2015**, *54*, 6398-6399; j) S. R. Waldvogel, S. Mohle, *Angew. Chem. Int. Ed*. **2015**, *54*, 6398-6399; k) P. Qian, M. Bi, Y. Wang, Z. Zha, Z. Wang, *J. Electrochem.* **2017**, *23*, 262-275.

[18] J. Jin, D. W. C. MacMillan, *Nature*. **2015**, *525*, 87-90.

[19] Due to the limited surface of the electrode used in our standard conditions A and B, readily commercial available other bulk electrode was applied instead, please see Figure S5.

[20] L. E. Sattler, C. J. Otten, G. Hilt, *Chem. Eur. J.* **2019**, 10.1002/chem.201904948.

[21] M. J. Frisch, G. W. Trucks, H. B. Schlegel, P. W. M. Gill, B. G. Johnson, M. A. Robb, J. R. Cheeseman, T. A. Keith, G. A. Petersson, J. A. Montgomery, K. Raghavachari, M. A. Allaham, V. G. Zakrzewski, J. V. Ortiz, J. B. Foresman, J. Cioslowski, B. B. Stefanov, A. Nanayakkara, M. Challacombe, C. Y. Peng, P. Y. Ayala, W. Chen, M. W. Wong, J. L. Andres, E. S. Replogle, R. omperts, R. L. Martin, D. J. Fox, J. S. Binkley, D. J. Defrees, J. Baker, J. P. Stewart, M. Head-Gordon, C. Gonzales, J. A. Pople, Gaussian 03, Revision D.01; Gaussian, Inc.: Pittsburgh, **2003**.

[22] S. D. Ross, M. Finkelstein, *J. Org. Chem.* **1969**, *34*, 2923-2927.

[23] Although NaI was obviated in some cases in condition A, the main factor for the chemoselectivity between C-N *vs* N-N bond formation was attributed to the current density employed.

[24] Both the starting material **1** and tetraarylhydrazine **3** was protonated in acidic condition, which will profoundly resulted in higher oxidative potential. Therefore, the anodic oxidation will be more difficult to be achieved.

[25] T. Ren, W. Xu, W. Zhang, X. Zhang, Z. Wang, Z. Xiang, L. Yuan, X. Zhang. *J. Am. Chem. Soc.* **2018**, *140*, 7716–7722.

10.1002/anie.202001510

WILEY-VCH

RESEARCH ARTICLE

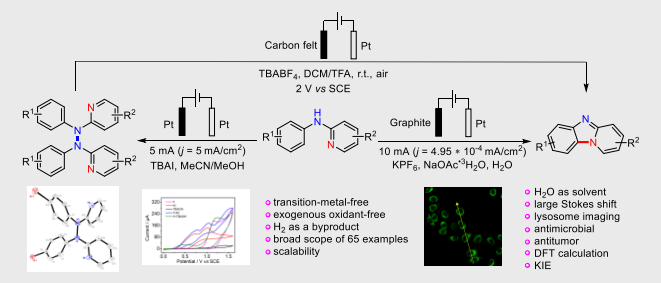

*Shide Lv,[†] Xiaoxin Han,[†] Jian-Yong Wang, Mingyang Zhou, Yanwei Wu, Li Ma, Liwei Niu, Wei Gao, Jianhua Zhou, Wei Hu, Yuezhi Cui, Jianbin Chen**

Page No. – Page No.

Tunable Electrochemical C-N *versus* N-N Bond Formation of Nitrogen-Centered Radicals Enabled by Dehydrogenative Dearomatization: Biological Applications

Tunable C-N *versus* N-N bond formation of nitrogen-centered radicals was achieved by an electrochemical dehydrogenative dearomatization strategy. Control experiments, DFT calculations, and investigations of the electrode material elucidated the origin of the chemoselectivity. The N-N product could be transformed into the C-N scaffold under complementary conditions, although the former was not the intermediate en route to the latter. Bioactivity assays demonstrated that pyrido[1,2-*a*]benzimidazoles displayed antimicrobial activity and cytotoxicity against human cancer cells. A large Stokes shift (approximately130 nm) and subcellular imaging were also demonstrated.